DEM construction based on HASM and related error analysis

CHEN Chuan-fa, YUE Tian-xiang, DU Zheng-ping, LU Yi-ming

Institute of Geographic Sciences and Natural Resources Research, Chinese Academy of Sciences, Beijing 100101, *China*

Abstract: In former researches, High Accuracy Surface Modelling (HASM) constructed based on the fundamental theory of surface is more accurate than the classical methods in DEM construction. In order to give HASM a full evaluation, this paper introduced terrain representation error (Etr), which was calculated by multi-resolution comparative analysis. Terrain representation model was built, which was regressed against resolution. The total DEM simulation error containing interpolation RMSE, Etr, etc., is calculated in terms of error propagation theory. Canonical surface and Dong-Zhi-Yuan in Gansu province of China were selected to validate the efficiency of our methods. The results showed that the method presented in this paper can give a full evaluation of DEM error. HASM can construct more accurate and higher resolution DEM than the classical methods.

Key words: surface modeling, interpolation, DEM, error analysis

CLC number: P237 **Document code:** A

Citation format: Chen C F, Yue T X, Du Z P and Lu Y M. 2010. DEM construction based on HASM and related error analysis. *Journal of Remote Sensing*, **14**(1): 080—089

1 INTRODUCTION

A digital elevation model (DEM) is a digital representation of terrain elevation as a function of geographic location (Yang *et al.*, 2007). DEM can be constructed with interpolation methods. DEMs are known to be fraught with errors of sampling, measurement and interpolation (Huang, 2000; Tang, 2000). DEM root mean square error (RMSE) is one of the indexes for DEM evaluation (Fisher, 1998; Gao, 1998). Terrain representation error (Etr) is always determined by DEM resolution under same terrain complexity. So the most important method for reducing DEM error is to improve the DEM accuracy and resolution (Gao, 1997).

High accuracy surface modelling (HASM) was constructed in terms of the fundamental theorem of surfaces (Yue *et al.*, 2007). Former researches indicated that HASM is more accurate than the classical methods including TIN, IDW, Spline and Kriging (Yue *et al.*, 2008), but when evaluating the DEM error, we only considered interpolation RMSE ignoring Etr.

In order to give DEM a comprehensive evaluation, the total DEM simulation error was presented in this paper, which is calculated in terms of error propagation theory. Canonical surface and Dong-Zhi-Yuan in Gansu were selected to comparatively analyze the total DEM errors of HASM and the classical methods.

2 THEORETICAL FORMULATION OF HASM

If a surface is a graph of a function $z=f(x, y)$, the Gauss equation sets can be formulated as,

$$\begin{cases} \dfrac{f^{n+1}_{i+1,j}-2f^{n+1}_{i,j}+f^{n+1}_{i-1,j}}{h^2}=(\Gamma^1_{11})^n_{i,j}\dfrac{f^n_{i+1,j}-f^n_{i-1,j}}{2h} \\ +\left(\Gamma^2_{11}\right)^n_{i,j}\dfrac{f^n_{i,j+1}-f^n_{i,j-1}}{2h}+\dfrac{L^n_{i,j}}{\sqrt{E^n_{i,j}+G^n_{i,j}-1}},(x_i,y_j)\in\Omega\setminus\partial\Omega \\ \dfrac{f^{n+1}_{i,j+1}-2f^{n+1}_{i,j}+f^{n+1}_{i,j-1}}{h^2}=(\Gamma^1_{22})^n_{i,j}\dfrac{f^n_{i+1,j}-f^n_{i-1,j}}{2h} \\ +\left(\Gamma^2_{22}\right)^n_{i,j}\dfrac{f^n_{i,j+1}-f^n_{i,j-1}}{2h}+\dfrac{N^n_{i,j}}{\sqrt{E^n_{i,j}+G^n_{i,j}-1}},(x_i,y_j)\in\Omega\setminus\partial\Omega \end{cases} \tag{1}$$

where, h represents DEM resolution

$$\begin{cases} E^n_{i,j}=1+\left(\dfrac{f^n_{i+1,j}-f^n_{i-1,j}}{2h}\right)^2 \\ F^n_{i,j}=\left(\dfrac{f^n_{i+1,j}-f^n_{i-1,j}}{2h}\right)\left(\dfrac{f^n_{i,j+1}-f^n_{i,j-1}}{2h}\right) \\ G^n_{i,j}=1+\left(\dfrac{f^n_{i,j+1}-f^n_{i,j-1}}{2h}\right)^2 \end{cases}$$

Received: 2008-06-30; **Accepted**: 2008-12-01

Foundation: China National Science Fund for Distinguished Young Scholars (No. 40825003), National High-tech R&D Program of Ministry of Science and Technology of the People's Republic of China (No. 2006AA12Z219), National Key Technologies R&D Program of Ministry of Science and Technology of the People's Republic of China (No. 2006BAC08B), Major Directivity Projects of Chinese Academy of Science (No. kzcx2-yw-429).

First author biography: CHEN Chuan-fa (1982—), male, PH.D. candidate, His research interest includes surface modelling and DEM uncertainty. He has published 3 papers. E-mail: chencf@lreis.ac.cn

$$\begin{cases} L_{i,j}^n = \dfrac{f_{i+1,j}^n - 2f_{i,j}^n + f_{i-1,j}^n}{\sqrt{1+\left(\dfrac{f_{i+1,j}^n - f_{i-1,j}^n}{2h}\right)^2 + \left(\dfrac{f_{i,j+1}^n - f_{i,j-1}^n}{2h}\right)^2}} \\ N_{i,j}^n = \dfrac{f_{i,j+1}^n - 2f_{i,j}^n + f_{i,j-1}^n}{\sqrt{1+\left(\dfrac{f_{i+1,j}^n - f_{i-1,j}^n}{2h}\right)^2 + \left(\dfrac{f_{i,j+1}^n - f_{i,j-1}^n}{2h}\right)^2}} \end{cases}$$

$$\begin{cases} (\Gamma_{11}^1)_{i,j}^n = [G_{i,j}^n(E_{i+1,j}^n - E_{i-1,j}^n) - 2F_{i,j}^n(F_{i+1,j}^n - F_{i-1,j}^n) + \\ \qquad F_{i,j}^n(E_{i,j+1}^n - E_{i,j-1}^n)]\{4[E_{i,j}^n G_{i,j}^n - (F_{i,j}^n)^2]h\}^{-1} \\ (\Gamma_{11}^2)_{i,j}^n = [2E_{i,j}^n(F_{i+1,j}^n - F_{i-1,j}^n) - E_{i-1,j}^n(E_{i,j+1}^n - E_{i,j-1}^n) - \\ \qquad F_{i,j}^n(E_{i+1,j}^n - E_{i-1,j}^n)]\{4[E_{i,j}^n G_{i,j}^n - (F_{i,j}^n)^2]h\}^{-1} \\ (\Gamma_{22}^1)_{i,j}^n = [2G_{i,j}^n(F_{i,j+1}^n - F_{i,j-1}^n) - G_{i,j}^n(G_{i+1,j}^n - G_{i-1,j}^n) - \\ \qquad F_{i,j}^n(G_{i,j+1}^n - G_{i,j-1}^n)]\{4[E_{i,j}^n G_{i,j}^n - (F_{i,j}^n)^2]h\}^{-1} \\ (\Gamma_{22}^2)_{i,j}^n = [E_{i,j}^n(G_{i,j+1}^n - G_{i,j-1}^n) - 2F_{i,j}^n(F_{i,j+1}^n - F_{i,j-1}^n) + \\ \qquad F_{i,j}^n(G_{i+1,j}^n - G_{i-1,j}^n)]\{4[E_{i,j}^n G_{i,j}^n - (F_{i,j}^n)^2]h\}^{-1} \end{cases}$$

The iterative simulation steps are summarized as follows: ① Computing the first and second fundamental coefficients E, F, G, L, N, as well as coefficients of HASM equations. ② For $n \geqslant 0$, we can get the DEM by solving the HASM equations. ③ The iterative process is repeated until simulation accuracy is satisfied.

3 ETR COMPUTATION

Fig.1 accounts for the existence of Etr on a 2D profile. The thick line ($\overline{ABC}$) represents the true ground surface, while A and C are two adjacent elevation points free from error. The elevation discrepancy between the elevation model surface ($\overline{AC}$) and the true surface ($\overline{ABC}$) is the Etr. α represents the slope at A; x is a variable, representing the distance between A and D. Therefore, Etr ($\overline{BE}$) can be formulated as,

$$\overline{BE} = \overline{BD} - \overline{ED} = x\tan\alpha - \frac{x^2\tan\alpha}{\overline{AF}} \tag{2}$$

Let first-order derivative of $\overline{BE}$ equal zero, we can obtain the location of D, where $\overline{BE}$ has the biggest value.

$$\begin{aligned} &\frac{\mathrm{d}(\overline{BE})}{\mathrm{d}x} = \tan\alpha - \frac{2x\tan\alpha}{\overline{AF}} = 0 \\ &x = \frac{\overline{AF}}{2} \end{aligned} \tag{3}$$

Eq. (3) revealed that at the middle point on $\overline{AF}$, it would be most possible to get the maximum Etr. In terms of this analysis, the maximum Etr between A and C can be computed with Eq. (4).

$$\mathrm{Etr}_{\max} = H_B - \frac{H_A + H_C}{2} \tag{4}$$

where H_A, H_B, H_C respectively represent the elevation values at A, B, C.

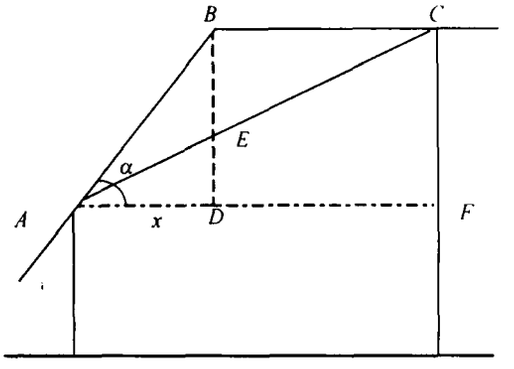

Fig. 1 2D profile model describing the Etr

In the 3D DEM, the maximum Etr within a grid can be expressed as,

$$\mathrm{Etr}_{\max} = H_C - \frac{H_{\mathrm{LU}} + H_{\mathrm{LB}} + H_{\mathrm{RU}} + H_{\mathrm{RB}}}{4} \tag{5}$$

where, H_C is the elevation value at the center of the grid; H_{LU}, H_{LB}, H_{RU} and H_{RB}, respectively, represent elevation values at the four corners of the grid.

Assuming the DEM resolution to be h, a 3×3 kernel window is employed to calculate the Etr with Eq. (6) (Fig. 2).

$$\mathrm{Etr}_{i,j} = H_{i,j} - \frac{H_{i+1,j+1} + H_{i+1,j-1} + H_{i-1,j-1} + H_{i-1,j+1}}{4} \tag{6}$$

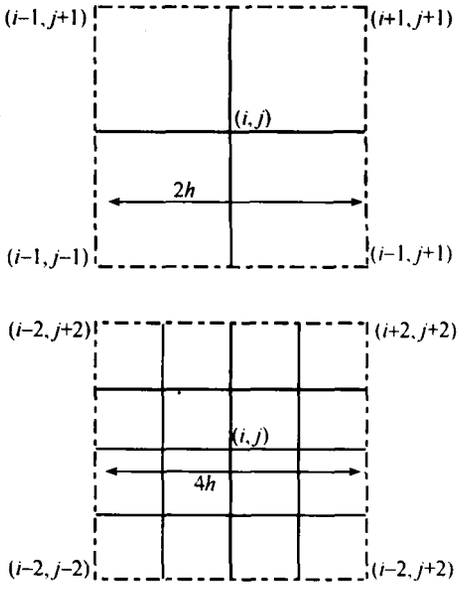

Fig. 2 Kernel window used to calculate Etr of DEM

If the kernel window moves through the whole DEM matrix cell by cell and computes the Etr value of each cell, we can derive an expected Etr matrix with the resolution of $2h$.

If the kernel window is extended to 5×5, 7×7, … , a set of DEM Etr matrices with the resolutions of $4h$, $6h$, …, can be derived respectively (Fig. 2). The root mean square error

(RMSE) of the Etr matrices can be calculated with Eq.(7).

$$\mathrm{RMSE}=\sqrt{\frac{\sum_{i=1,j=1}^{i=\mathrm{Row},j=\mathrm{Colum}}\mathrm{Etr}_{i,j}^2}{\mathrm{Row}\times\mathrm{Colum}}} \tag{7}$$

where Row, Colum respectively represent the row and column of Etr matrix.

Therefore, in terms of error propagation theorem, the total DEM error (m_D) can be formulated as,

$$m_D=\sqrt{m_\mathrm{I}^2+m_\mathrm{T}^2+m_\mathrm{S}^2} \tag{8}$$

where m_I, m_T, m_S represent interpolation RMSE, Etr and sampling RMSE respectively. The total DEM error can be regarded as the first criterion for assessing DEM accuracy.

4 HASM ERROR ANALYSIS

4.1 A numerical test

$z=2\sin(\pi x)\sin(\pi y)+1$, the canonical surface was employed to comparatively analyze the DEM error, thus the "true" output value can be pre-determined to avoid uncertainty caused by uncontrollable data errors. Its computational domain is [0,1]× [0,1]. The RMSE of Etr matrices with different resolutions were calculated. The results were shown in Table 1. The regression model that related the resolution and Etr was generated with SPSS, which appears to have a non-linear (quadratic) correlation (Fig.3 and Eq.(9)). Variance analysis showed that the curve through the sampling points completely indicates that the regression model has a good fitness (F=8541954, P=0).

$$\mathrm{RMSE}=1.52\times10^{-6}-0.001h+2.516h^2;R^2=1 \tag{9}$$

In addition to the newly developed HASM, there are many other methods of surface modelling, which are widely used in various GIS applications, including IDW, Spline and Kriging.

Table 1 Terrain representation errors of canonical surface (h=1/800)

Resolution	$2h$	$4h$	$6h$	$8h$	$10h$	$12h$	$14h$	$16h$	$18h$	$20h$
RMSE/10^{-5}	1.5	6.2	13.9	24.8	38.8	55.9	76.2	99.7	126.3	156.1

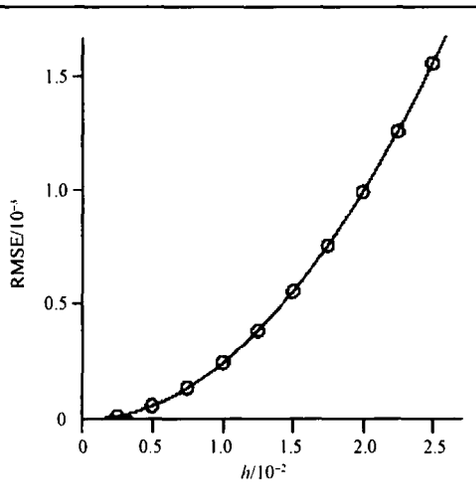

Fig. 3 Etr regression model of canonical surface

These four models were employed to comparatively analyze DEM errors. In the computational domain, 25 points were used as the sampling data. All the classical interpolation methods were performed using the module of 3D analyst in ArcGIS 9.2 with the default parameters. The interpolation RMSE was calculated with Eq.(10). The results were shown in Table 2.

$$\mathrm{RMSE}=\sqrt{\frac{\sum_{i=1}^{\mathrm{Row}}\sum_{j=1}^{\mathrm{Colum}}(f_{i,j}-\mathrm{sf}_{i,j})^2}{\mathrm{Row}\times\mathrm{Colum}}}; \tag{10}$$

where, Row, Colum respectively represent the row and column of the lattices matrix; $\mathrm{sf}_{i,j}$, $f_{i,j}$ represent the simulation value and true value at the lattice (i,j) respectively.

Table 2 Interpolation RMSE under different methods

Resolution	HASM/10^{-4}	IDW	Spline	Kriging
1/8	9.72	0.75	0.21	0.37
1/16	5.61	0.45	0.29	0.51
1/32	3.67	0.53	0.34	0.58
1/64	4.57	0.57	0.36	0.62

Based on Eq. (8), the total DEM errors were calculated (Table 3).

Table 3 Total DEM error under different methods

Resolution	HASM/10^{-4}	IDW	Spline	Kriging
1/8	392	0.75	0.21	0.37
1/16	98	0.45	0.29	0.51
1/32	25	0.53	0.34	0.58
1/64	8	0.57	0.36	0.62

Results indicated that HASM is more obviously affected by Etr than the classical methods (Table 2 and 3). Although Etr has little influence on the classical methods, HASM is still more accurate than the classical methods. When the resolution is 1/64, the HASM interpolation error is bigger than that of resolution of 1/32 (Table 2). But when taking the Etr into account (Table 3), the HASM total error becomes smaller with the resolution increasing (grid cell size becoming smaller), which indicates that if ignoring the impact of resolution on the terrain representation, we might obtain wrong conclusions. Considering all DEMs derived from the classical methods, the total DEM error increases as the grid cell size decreases. Therefore, under the same sampling data and any resolution, HASM is more accurate than the classical methods.

4.2 Real-world example

Dong-Zhi-Yuan experimental station was selected for this study. It was located in Gansu province of China with area of 2260km^2. The geographic coordinates of its central point are 107.88°E and 36.03°N. One of the topographic maps was utilized in this study to derive DEMs. The topographic map with

scale 1 : 5000 has a 25m-vertical-interval between each contour line. Its elevations vary from 1 195m to 1 530m. The scanned topographic map was enlarged three times in order to enhance the digitization accuracy. Contours were traced using the module of Editor in ArcGIS 9.2. After that, the elevations were sampled from the contours using data management tools. The elevations were interpolated with resolution of 5 m. RMSE of Etr matrices with different analysis resolutions were calculated. The results were shown in Table 4. The regression model that related the resolution and Etr was generated with SPSS (Fig. 4 and Eq.(11)), which appears to have linear correlation. Variance analysis shows that the curve through the sampling points completely indicates that the regression model has a good fitness ($F = 44713.618$, $P = 0$).

$$\mathrm{RMSE} = 0.134h + 1.738; R^2 = 1 \tag{11}$$

Table 4 Terrain representation error of Dong-Zhi-Yuan/m

Resolution	10	20	30	40	50	60	70	80	90	100
RMSE	3.00	4.50	5.81	7.10	8.40	9.70	11.05	12.42	13.8	15.15

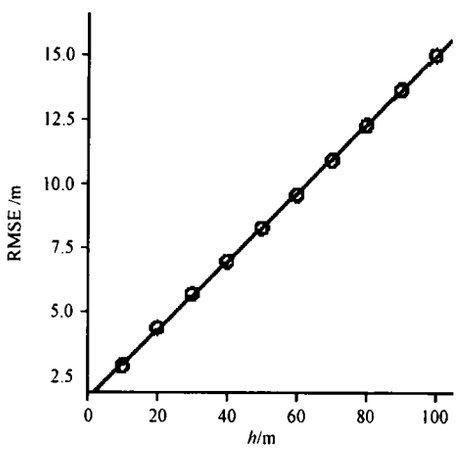

Fig. 4 Etr regression model of Dong-Zhi-Yuan

The interpolation accuracy of terrain representation was evaluated against RMSE at 30% randomly selected elevations as check points (Table 5). Assuming the DEM sampling error to be zero, the corresponding total DEM error was calculated with Eq.(8) (Table 6).

Table 5 indicated that when the resolution is 20m, HASM has a bigger interpolation accuracy loss, which might be caused by the location differences between the sampling points and the corresponding central points of lattices of the simulated surfaces. When taking Etr into account, the total DEM error of

Table 5 Interpolation RMSE under different methods in Dong-Zhi-Yuan/m

Resolution	HASM	IDW	Spline	Kriging
30	9.33	13.72	13.05	13.96
20	9.60	11.79	10.41	12.64
10	8.86	11.14	9.69	12.28
5	8.79	10.80	9.18	12.15

Table 6 Total DEM error under different methods in Dong-Zhi-Yuan/m

Resolution	HASM	IDW	Spline	Kriging
30	10.97	14.88	14.26	15.10
20	10.56	12.59	11.30	13.39
10	9.40	11.56	10.16	12.67
5	9.11	11.06	9.49	12.39

HASM decreases with the resolution increasing (Table 6). So only taking interpolation error as the criterion for assessing DEM accuracy, we might not give HASM a comprehensive evaluation. Under any resolution, HASM is more accurate than the classical methods. HASM may be an alternative for DEM construction.

5 CONCLUSIONS

In order to give DEM a full evaluation, Etr was presented and regression model that relates Etr and DEM resolution was generated with SPSS. Total DEM simulation error was calculated in terms of error propagation theory. We selected the canonical surface and Dong-Zhi-Yuan to analyze the total DEM simulation error of HASM and the classical methods including IDW, Spline and Kriging. Numerical test and real-world example showed that when taking Etr into account, we can give HASM a full evaluation. HASM is more accurate than the classical methods, which can be considered as an alternative for DEM construction.

HASM has a huge computation cost because it must use an equation set for simulating each lattice of a surface. An adaptive simulation approach with grid selection strategies is highly significant for HASM, which is a very desirable feature for an accurate analysis and an efficient simulation (Berger, 1989; Jessee *et al.*, 1998). Adaptive method for HASM concentrates computational effort where it is most needed, which may reduce much simulation cost and volume storage than global simulation (Martin, 1998; Ekevid *et al.*, 2004).

REFERENCES

Berger M J and Rigoutsos I. 1991. An algorithm for point clustering and grid generation. *IEEE Transactions on Systems, Man and Cybernetics*, **21**(5): 1278—1286

Chen C F, Yue T X and Lu Y M. 2009. Method of reducing HASM boundary error. *Journal of Remote Sensing*, **13**(3): 458—462

Chen C F, Yue T X, Zhang Z J and Du Z P. 2008. Height anomaly surface modelling based on height accurate surface model. *Journal of Geodesy and Geodynamics*, **28**(5): 82—86

Darnell A R, Tate N J and Brunsdon C. 2008. Improving user assessment of error implications in digital elevation models. *Computers,*

Environment and Urban Systems, **32**(4): 268—277

Li Z. 1991. Effect of check points on the reliability of DTM accuracy estimates obtained form experimental tests. *Photogram Metric Engineering and Remote Sensing*, **57**(10): 1331—1340

Martin D F and Colella P. 2000. A cell-centered adaptive projection method for the incompressible Euler equations. *Journal of Computational Physics*, **163**(2): 271—312

Mei X M and Huang J Z. 2003. Differential Geometry. Beijing: Higher Education Press

Tang G A, Long J Y and Chen Z J. 2001. A simulation on the accuracy of DEM terrain representation. *Acta Geodaetica et Cartographica Sinica*, **30**(4): 361—365

Tang G A. 2000. A research on the Accuracy of Digital Elevation Models. Beijing: Science Press

Yang Q K. 2007. Improving a digital elevation model by reducing source data errors and optimizing interpolation algorithm parameters: An example in the Loess Plateau, China. *International Journal of Applied Earth Observation and Geoinformation*, **9**: 235—246

Yue T X and Du Z P. 2005. High precision surface modeling: a core module of new generation CAD and GIS. *Progress in Natural Science*, **15**(4): 73—82

Yue T X and Du Z P. 2006. High accuracy modeling and comparative analysis of its errors. *Progress in Natural Science*, **16**(18): 986—991

Yue T X, Du Z P and Liu J Y. 2004. High precision surface modeling and error analysis. *Progress in Natural Science*, **14**(2): 83—89

Yue T X, Du Z P and Song D J. 2007. A new method of surface modelling and its application to DEM construction. *Geomorphology*, **91**: 161—172

基于高精度曲面模型的 DEM 构建与误差分析

陈传法，岳天祥，杜正平，卢毅敏

中国科学院 地理科学与资源研究所，北京 100101

摘 要： 引入地形表达误差(terrain representation error, Etr)，选择标准曲面和甘肃省董志塬地区作为研究对象，利用窗口分析法实现 Etr 的提取；用统计分析法得出 Etr 随网格分辨率变化的回归方程；根据误差传播定律计算 DEM 中误差。数值结果表明，该方法能更准确的计算 HASM 生成的 DEM 精度；相同的采样数下，HASM 较传统方法(IDW, Spline 和 Kriging)能生成更高精度和分辨率的 DEM。在难以获取已知数据的地区，HASM 提供了生成相对准确 DEM 的高效工具。

关键词： 曲面建模，插值，DEM，误差分析

中图分类号： P237 **文献标识码：** A

引用格式： 陈传法，岳天祥，杜正平，卢毅敏. 2010. 基于高精度曲面模型的 DEM 构建与误差分析. 遥感学报，14(1): 080—089
Chen C F, Yue T X, Du Z P and Lu Y M. 2010. DEM construction based on HASM and related error analysis. *Journal of Remote Sensing*, 14(1): 080—089

1 引 言

数字高程模型(digital elevation model, DEM)是对地球表面地形地貌的一种离散的数字表达(Yang, 2007)。构建 DEM 常用方法之一是利用插值技术对已知数据内插完成。DEM 精度表述为利用已知数据建立的 DEM 对真实地面描述的准确程度，DEM 误差是衡量 DEM 精度的重要指标(Li, 1991)。DEM 误差可分为高程采样误差、插值误差和地形表达误差(terrain representation error, Etr)(Tang, 2000; Damell 等, 2008)。在地形复杂度一定的情况下，Etr 受 DEM 网格分辨率的影响(汤国安等, 2001)。如何利用有限的采样数据获取高精度和高分辨率的 DEM 是降低 DEM 误差的关键技术。

有曲面论定律可知，曲面有第一基本量和第二基本量确定(梅向明等, 2003)，据此，建立了高精度曲面模型(high accuracy surface modelling, HASM)(岳天祥等, 2004, 2005)。HASM 以高斯方程作为构建曲面的基本方程，将已知采样数据作为高斯方程的约束条件，利用最小二乘求算构建的方程就可以得到高精度曲面。以往研究表明，HASM 插值精度较传统方法提高了多个数量级，但对 DEM 误差评价时仅考虑了插值误差(岳天祥等, 2006; 陈传法等, 2009)。

为了合理验证 HASM 构建的 DEM 误差，本文选择标准曲面和甘肃省董志塬作为研究对象，对 DEM 误差评价中引入 Etr，并比较 HASM 与 GIS 常用的插值方法(IDW, Spline 以及 Kriging)获取的 DEM 误差。

2 HASM 原理

设曲面表达式为 $z=f(x, y)$，$\{(x_i, y_j)\}$是对计算区域 Ω 进行均匀正交剖分产生的网格，则 HASM 的最佳迭代模拟方程为(岳天祥等, 2004)

$$\begin{cases} \dfrac{f_{i+1,j}^{n+1}-2f_{i,j}^{n+1}+f_{i-1,j}^{n+1}}{h^2}=(\Gamma_{11}^1)_{i,j}^n\dfrac{f_{i+1,j}^n-f_{i-1,j}^n}{2h} \\ +\left(\Gamma_{11}^2\right)_{i,j}^n\dfrac{f_{i,j+1}^n-f_{i,j-1}^n}{2h}+\dfrac{L_{i,j}^n}{\sqrt{E_{i,j}^n+G_{i,j}^n-1}},(x_i,y_j)\in\Omega\backslash\partial\Omega \\ \dfrac{f_{i,j+1}^{n+1}-2f_{i,j}^{n+1}+f_{i,j-1}^{n+1}}{h^2}=(\Gamma_{22}^1)_{i,j}^n\dfrac{f_{i+1,j}^n-f_{i-1,j}^n}{2h} \\ +\left(\Gamma_{22}^2\right)_{i,j}^n\dfrac{f_{i,j+1}^n-f_{i,j-1}^n}{2h}+\dfrac{N_{i,j}^n}{\sqrt{E_{i,j}^n+G_{i,j}^n-1}},(x_i,y_j)\in\Omega\backslash\partial\Omega \end{cases} \tag{1}$$

收稿日期： 2008-06-30；**修订日期：** 2008-12-01

基金项目： 国家杰出青年科学基金(编号：40825003)，国家高新技术发展计划(编号：2006AA12Z219)，国家科技支撑计划课题(编号：2006BAC08B)和中国科学院知识创新工程重要方向项目(编号：kzcx2-yw-429)。

第一作者简介： 陈传法(1982—)，男，山东沂源人，中国科学院地理科学与资源研究所在读博士研究生，目前主要从事曲面建模和 DEM 不确定性研究。E-mail: chencf@lreis.ac.cn。

式中，h 为网格分辨率；n 为迭代次数；E, F, G 为曲面第一基本量；L, N 为曲面第二基本量；Γ_i^k, $(i=11,22,k=1,2)$ 为第 2 类克里斯托费尔符号，它们表达式为：

$$\begin{cases} E_{i,j}^n = 1+\left(\dfrac{f_{i+1,j}^n - f_{i-1,j}^n}{2h}\right)^2 \\ F_{i,j}^n = \left(\dfrac{f_{i+1,j}^n - f_{i-1,j}^n}{2h}\right)\left(\dfrac{f_{i,j+1}^n - f_{i,j-1}^n}{2h}\right) \\ G_{i,j}^n = 1+\left(\dfrac{f_{i,j+1}^n - f_{i,j-1}^n}{2h}\right)^2 \end{cases}$$

$$\begin{cases} L_{i,j}^n = \dfrac{f_{i+1,j}^n - 2f_{i,j}^n + f_{i-1,j}^n}{\sqrt{1+\left(\dfrac{f_{i+1,j}^n - f_{i-1,j}^n}{2h}\right)^2 + \left(\dfrac{f_{i,j+1}^n - f_{i,j-1}^n}{2h}\right)^2}} \\ N_{i,j}^n = \dfrac{f_{i,j+1}^n - 2f_{i,j}^n + f_{i,j-1}^n}{\sqrt{1+\left(\dfrac{f_{i+1,j}^n - f_{i-1,j}^n}{2h}\right)^2 + \left(\dfrac{f_{i,j+1}^n - f_{i,j-1}^n}{2h}\right)^2}} \end{cases}$$

$$\begin{cases} (\Gamma_{11}^1)_{i,j}^n = [G_{i,j}^n(E_{i+1,j}^n - E_{i-1,j}^n) - 2F_{i,j}^n(F_{i+1,j}^n - F_{i-1,j}^n) + \\ \qquad F_{i,j}^n(E_{i,j+1}^n - E_{i,j-1}^n)]\{4[E_{i,j}^n G_{i,j}^n - (F_{i,j}^n)^2]h\}^{-1} \\ (\Gamma_{11}^2)_{i,j}^n = [2E_{i,j}^n(F_{i+1,j}^n - F_{i-1,j}^n) - E_{i-1,j}^n(E_{i,j+1}^n - E_{i,j-1}^n) - \\ \qquad F_{i,j}^n(E_{i+1,j}^n - E_{i-1,j}^n)]\{4[E_{i,j}^n G_{i,j}^n - (F_{i,j}^n)^2]h\}^{-1} \\ (\Gamma_{22}^1)_{i,j}^n = [2G_{i,j}^n(F_{i,j+1}^n - F_{i,j-1}^n) - G_{i,j}^n(G_{i+1,j}^n - G_{i-1,j}^n) - \\ \qquad F_{i,j}^n(G_{i,j+1}^n - G_{i,j-1}^n)]\{4[E_{i,j}^n G_{i,j}^n - (F_{i,j}^n)^2]h\}^{-1} \\ (\Gamma_{22}^2)_{i,j}^n = [E_{i,j}^n(G_{i,j+1}^n - G_{i,j-1}^n) - 2F_{i,j}^n(F_{i,j+1}^n - F_{i,j-1}^n) + \\ \qquad F_{i,j}^n(G_{i+1,j}^n - G_{i-1,j}^n)]\{4[E_{i,j}^n G_{i,j}^n - (F_{i,j}^n)^2]h\}^{-1} \end{cases}$$

利用 HASM 构建 DEM 主要步骤为：①利用已知采样点计算第一基本量 E,F,G，第二基本量 L, N 和 HASM 系数；②将公式(1)右端计算值作为已知量，左端变量作为未知量，求算 HASM 方程；③将算出的新值作为已知值，重复①—②计算过程直到满足精度要求。

3 地形表达误差(Etr)计算

Etr 定义为当采样误差和插值误差为零时，模拟地面与实际地面的差异。如图 1，$\overline{ABC}$ 表示实际地面的剖面，$\overline{AC}$ 表示线性结构的剖面，则 $\overline{BE}$ 为因线性插值而带来的 Etr。令 α 为点 A 处的坡度值，则：

$$\overline{BE} = \overline{BD} - \overline{ED} = x\tan\alpha - \frac{x^2\tan\alpha}{\overline{AF}} \tag{2}$$

令 $\overline{BE}$ 的一阶导数为 0，则 $\overline{BE}$ 取最大值时 B 点的位置可由(3)式计算：

$$\frac{\mathrm{d}(\overline{BE})}{\mathrm{d}x} = \tan\alpha - \frac{2x\tan\alpha}{\overline{AF}} = 0 \tag{3}$$

得出，$x=\dfrac{\overline{AF}}{2}$，表明在 $\overline{AC}$ 的中点位置线性插值带来的 Etr 最大。同理，双线性插值在 4 个点的中点位置 Etr 最大，因此可以利用窗口分析法(Tang, 2000)计算 Etr。窗口分析法基本思想为：设 H_a, H_b, H_c, H_d, H_o 为对应地面点 A,B,C,D 以及该 4 个点中点 O 的高程真值，则 Etr 可以表达为：$\mathrm{Etr}=H_o-(H_a+H_b+H_c+H_d)/4$。对于分辨率为 h 的栅格 DEM，利用 3×3 窗口计算第 (i,j) 点的 Etr 公式为(图 2)：$\mathrm{Etr}_{i,j}=H_{i,j}-\dfrac{H_{i-1,j-1}+H_{i-1,j+1}+H_{i+1,j-1}+H_{i+1,j+1}}{4}$。显然 3×3 窗口

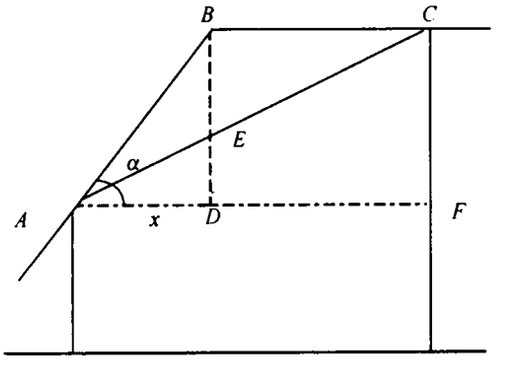

图 1 线性表达带来的地形表达误差示意图

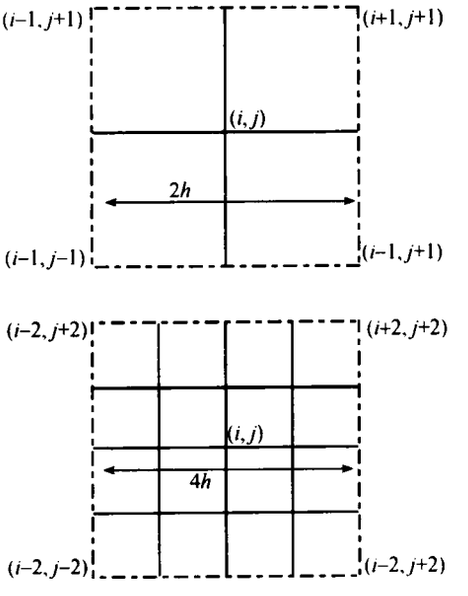

图 2 窗口分析法计算 Etr 示意图

计算的 Etr 分辨率为 $2h$。顺序移动该窗口计算整个 DEM 的 Etr，可以得出对应分辨率的误差矩阵。同理，分析窗口扩大到 5×5, 7×7, …，可以计算分辨率为 $4h$, $6h$, …, 的误差矩阵。

Etr 使用中误差(RMSE)衡量，计算公式为：

$$\mathrm{RMSE}=\sqrt{\frac{\sum_{i=1,j=1}^{i=\mathrm{Row},j=\mathrm{Colum}}\mathrm{Etr}_{i,j}^2}{\mathrm{Row}\times\mathrm{Colum}}} \tag{4}$$

式中，Row, Colum 分别为 Etr 矩阵的行数和列数；$\mathrm{Etr}_{i,j}$ 为 Etr 矩阵中第 i 行 j 列的值。

4 HASM 实例分析

4.1 标准曲面研究

选择标准曲面 $z=2\sin(\pi x)\sin(\pi y)+1$ 为研究对象，模拟区域为 $[0,1]\times[0,1]$。利用窗口分析法计算 Etr，计算结果如表 1。图 3 显示 Etr(RMSE)随分辨率的降低而增大且呈明显的二次线性相关关系，回归方程为：

$$\mathrm{RMSE}=1.52\times10^{-6}-0.001h+2.516h^2;R^2=1 \tag{5}$$

作拟合优度检验，方差分析表明：F=8541954, P=0，表明拟合曲线通过已知样点，拟合结果准确。

表 1 标准曲面地形表达误差(h=1/800)

分辨率	$2h$	$4h$	$6h$	$8h$	$10h$	$12h$	$14h$	$16h$	$18h$	$20h$
RMSE/10^{-5}	1.5	6.2	13.9	24.8	38.8	55.9	76.2	99.7	126.3	156.1

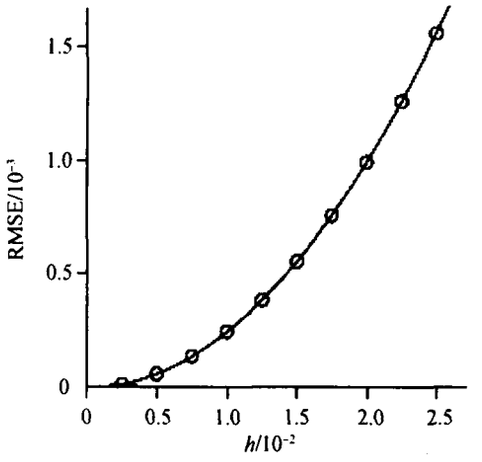

图 3 标准曲面 Etr 随分辨率变化曲线

均匀选择 25 个点作为已知采样点，用 HASM 以及 GIS 插值方法(IDW, Spline 和 Kriging)分别生成不同分辨率的 DEM。由于各个网格点的真值可以通过曲面方程计算，因此可以准确计算不同分辨率 DEM 的插值中误差，计算结果如表 2。

由于采样误差为零，根据误差传播定律，DEM 中误差 m_D 的计算公式为：

$$m_D=\sqrt{m_I^2+m_T^2} \tag{6}$$

式中，m_I 为插值中误差，m_T 为 Etr。借助公式(6)求算的 DEM 中误差结果如表 3。

表 2 各种插值方法获取的 DEM 插值中误差

分辨率	HASM/10^{-4}	IDW	Spline	Kriging
1/8	9.72	0.75	0.21	0.37
1/16	5.61	0.45	0.29	0.51
1/32	3.67	0.53	0.34	0.58
1/64	4.57	0.57	0.36	0.62

表 3 各种插值方法获取的 DEM 中误差

分辨率	HASM/10^{-4}	IDW	Spline	Kriging
1/8	392	0.75	0.21	0.37
1/16	98	0.45	0.29	0.51
1/32	25	0.53	0.34	0.58
1/64	8	0.57	0.36	0.62

从表 2、表 3 可见，HASM 受 Etr 影响较大；由于 IDW, Spline 和 Kriging 的插值中误差远大于 Etr，所以它们的 DEM 中误差几乎没有受 Etr 影响，但仍远大于 HASM。如果没有考虑 Etr(表 2)，当模拟分辨率为 1/64 时，HASM 插值中误差大于 1/32，但由于分辨率越高，Etr 越小，综合考虑，HASM 在分辨率为 1/64 时的 DEM 中误差小于分辨率为 1/32(表 3)。因此，如果忽略 Etr 判断 DEM 中误差是不准确的。进一步分析表 3 可见，随着网格分辨率的提高，HASM 的 DEM 中误差逐渐变小，而传统的插值方法除 IDW 在分辨率为 1/16 时 DEM 中误差稍有降低外，均成增大趋势，这表明，在相同的采样数据条件下，HASM 较传统的方法能生成更高精度和分辨率的 DEM。

4.2 董志塬试验区研究

董志塬位于甘肃省东部的庆阳市腹部，介于 E107°39′—108°05′，N35°28′—35°40′，总面积达 2778km^2，平均海拔 1300—1400m。有 13 条较大河沟呈辐射状向塬心伸入，分割塬面成多数碎块。一般沟壑深 150—200m，大小沟壑占总面积的 61%，荒坡又占沟壑面积 57%。本文数据来自 1: 5000 地形图，等高距为 25m。利用所有已知数据生成分辨率为 5m 的 DEM，并用窗口分析法计算 Etr，计算结果

如表 4。图 4 显示 Etr 随分辨率的降低而增大并呈线性相关关系，回归方程为：

$$RMSE = 0.134h + 1.738 \ (R^2 = 1) \qquad (7)$$

作拟合优度检验，方差分析表明：F=44713.618, P=0，拟合效果非常好。

为了计算插值中误差，我们随机选择 70%数据作为已知点生成不同分辨率的 DEM，用 30%数据作为检核点进行交叉验证。各种方法生成的不同分辨率 DEM 插值中误差如表 5，在不考虑采样误差的前提下，根据公式(6)计算的 DEM 中误差如表 6。

从表 5 可见，网格分辨率从 30m 提高到 5m 时，HASM 插值中误差先增大后降低，而传统的插值方法的插值中误差一直降低，但它们的插值精度始终小于 HASM。考虑 Etr 时，如表 6 所示，随着网格分辨率的提高，HASM生成的DEM中误差呈下降趋势，且小于传统的插值方法。因此，如果不考虑 Etr 而对 HASM 生成的 DEM 误差进行评价并不准确；HASM 较传统的方法能生成更高精度的 DEM。

表 4 董志塬地形表达误差/m

分辨率	10	20	30	40	50	60	70	80	90	100
RMSE	3.00	4.50	5.81	7.10	8.40	9.70	11.05	12.42	13.8	15.15

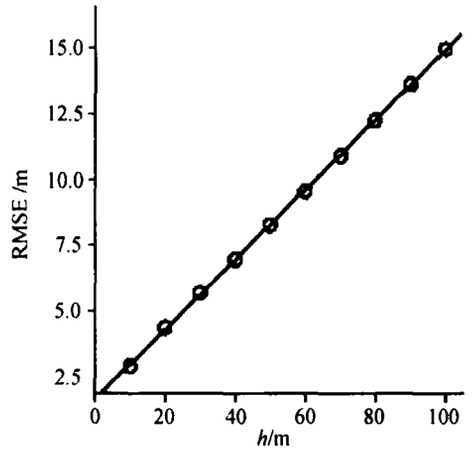

图 4 董志塬 Etr 随分辨率变化曲线

表 5 各种方法获取的 DEM 插值中误差/m

分辨率	HASM	IDW	Spline	Kriging
30	9.33	13.72	13.05	13.96
20	9.60	11.79	10.41	12.64
10	8.86	11.14	9.69	12.28
5	8.79	10.80	9.18	12.15

表 6 各种插值方法获取的 DEM 中误差/m

分辨率	HASM	IDW	Spline	Kriging
30	10.97	14.88	14.26	15.10
20	10.56	12.59	11.30	13.39
10	9.40	11.56	10.16	12.67
5	9.11	11.06	9.49	12.39

5 结 论

本文选择标准曲面和董志塬地区作为研究对象，充分考虑地形表达误差的影响，利用窗口分析法实现 Etr 的提取，并用统计分析法得出 Etr 随网格分辨率变化的回归方程。误差分析表明，Etr 对 HASM 生成的 DEM 精度影响较大；相同的采样数下，HASM 较传统的方法能构建高精度和高分辨率的 DEM。在难以获取已知数据的地区，HASM 提供了构建相对准确 DEM 的高效工具。

由于HASM需要对每个网格点建立一个偏微分方程，计算量巨大(Yue 等, 2007; 陈传法等, 2008)。自适应曲面建模可以根据模拟区域的地形复杂度自动调整网格分辨率，从而有效的减少网格点数，提高 HASM 运算速度(Berger 等, 1991; Martin & Colella, 2000)。因此我们下一步的工作是构建具有适应性质的高精度曲面模型。

REFERENCES

Berger M J and Rigoutsos I. 1991. An algorithm for point clustering and grid generation. *IEEE Transactions on Systems, Man and Cybernetics*, **21**(5): 1278—1286

Chen C F, Yue T X and Lu Y M. 2009. Method of reducing HASM boundary error. *Journal of Remote Sensing*, **13**(3): 458—468

Chen C F, Yue T X, Zhang Z J and Du Z P. 2008. Height anomaly surface modelling based on height accurate surface model. *Journal of Geodesy and Geodynamics*, **28**(5): 82—86

Darnell A R, Tate N J and Brunsdon C. 2008. Improving user assessment of error implications in digital elevation models. *Computers, Environment and Urban Systems*, **32**(4): 268—277

Li Z. 1991. Effect of check points on the reliability of DTM accuracy estimates obtained form experimental tests. *Photogram Metric Engineering and Remote Sensing*, **57**(10): 1331—1340

Martin D F and Colella P. 2000. A cell-centered adaptive projection method for the incompressible Euler equations. *Journal of*

Computational Physics, **163**(2): 271—312

Mei X M and Huang J Z. 2003. Differential Geometry. Beijing: Higher Education Press

Tang G A, Long J Y and Chen Z J. 2001. A simulation on the accuracy of DEM terrain representation. *Acta Geodaetica et Cartographica Sinica*, **30**(4): 361—365

Tang G A. 2000. A research on the Accuracy of Digital Elevation Models. Beijing: Science Press

Yang Q K. 2007. Improving a digital elevation model by reducing source data errors and optimizing interpolation algorithm parameters: An example in the Loess Plateau, China. *International Journal of Applied Earth Observation and Geoinformation*, **9**: 235—246

Yue T X and Du Z P. 2005. High precision surface modeling: a core module of new generation CAD and GIS. *Progress in Natural Science*,**15**(4): 73—82

Yue T X and Du Z P. 2006. High accuracy modeling and comparative analysis of its errors. *Progress in Natural Science*, **16**(18): 986—991

Yue T X, Du Z P and Liu J Y. 2004. High precision surface modeling and error analysis. *Progress in Natural Science*, **14**(2): 83—89

Yue T X, Du Z P and Song D J. 2007. A new method of surface modelling and its application to DEM construction. *Geomorphology*, **91**: 161—172

附中文参考文献

陈传法, 岳天祥, 卢毅敏. 2009. 高精度曲面建模应用中边界误差解决方案. 遥感学报, **13**(3): 458—468

陈传法, 岳天祥, 张照杰, 杜正平. 2008. 基于高精度曲面模型的高程异常曲面模拟. 大地测量与地球动力学, **28**(5): 82—86

梅向明, 黄敬之. 2003. 微分几何. 北京: 高等教育出版社

汤国安, 龚健雅, 陈正江. 2001. 数字高程模型地形描述精度量化模拟研究. 测绘学报, **30**(4): 361—365

岳天祥, 杜正平. 2006. 高精度曲面建模与经典模型的误差比较分析. 自然科学进展, **16**(18): 986—991

岳天祥, 杜正平, 刘纪远. 2004. 高精度曲面建模与误差分析. 自然科学进展, **14**(2): 83—89

岳天祥, 杜正平. 2005. 高精度曲面建模: 新一代 GIS 与 CAD 的核心模块. 自然科学进展, **15**(4): 73—82